Correlation effects in side-coupled quantum dots

2007 J. Phys.: Condens. Matter 19 255205

(http://iopscience.iop.org/0953-8984/19/25/255205)

IOP PUBLISHING JOURNAL OF PHYSICS: CONDENSED MATTER

J. Phys.: Condens. Matter **19** (2007) 255205 (12pp) doi:10.1088/0953-8984/19/25/255205

Correlation effects in side-coupled quantum dots

R Žitko[1] **and J Bonča**[1,2]

[1] J Stefan Institute, Jamova 39, SI-1000 Ljubljana, Slovenia
[2] Department of Physics, FMF, University of Ljubljana, Jadranska 19, SI-1000 Ljubljana, Slovenia

E-mail: rok.zitko@ijs.si and janez.bonca@ijs.si

Received 31 August 2006, in final form 25 September 2006
Published 30 May 2007
Online at stacks.iop.org/JPhysCM/19/255205

Abstract

Using Wilson's numerical renormalization group (NRG) technique, we compute zero-bias conductance and various correlation functions of a double quantum dot (DQD) system. We present different regimes within a phase diagram of the DQD system. By introducing a negative Hubbard U on one of the quantum dots, we simulate the effect of electron–phonon coupling and explore the properties of the coexisting spin and charge Kondo state. In a triple quantum dot (TQD) system, a multi-stage Kondo effect appears where localized moments on quantum dots are screened successively at exponentially distinct Kondo temperatures.

(Some figures in this article are in colour only in the electronic version)

1. Introduction

The development of nanotechnology has stimulated studies of transport through coupled quantum dots systems, where at very low temperatures Kondo physics as well as magnetic interactions play an important role. A double-dot system represents the simplest generalization of a single-dot system which has been extensively studied in the past. Recent experiments demonstrate that similar realistic devices can be constructed [1–4], which enables direct experimental investigations of the competition between the Kondo effect and the exchange interaction between localized moments on the dots. One manifestation of this competition is a two-stage Kondo effect that has recently been predicted in multilevel quantum dot systems with explicit exchange interaction coupled to one or two conduction channels [5, 6]. Experimentally, it manifests itself as a sharp drop in the conductance versus gate voltage $G(V_G)$ [7] or as non-monotonic dependence of the differential conductance versus drain–source voltage $dI/dV_{ds}(V_{ds})$ [8].

Another line of research of correlation effects in quantum dots concerns the influence of localized phonon modes on electron transport through quantum dots and molecules. The influence of a strong, localized electron–phonon interaction [9] can be simulated by the introduction of an effective negative-U Anderson model. In such a system the *charge Kondo*

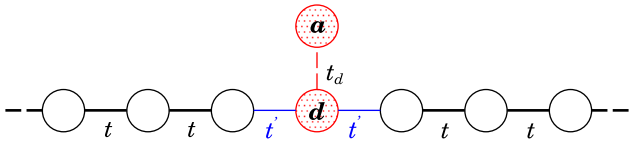

Figure 1. Side-coupled configuration of quantum dots.

effect leads to screening of charge fluctuations on the localized impurity by low-frequency pair fluctuations in the leads [10]. It has recently been shown that in the case of large electron–phonon coupling the original single-impurity Anderson model, coupled to local phonon degrees of freedom, can be mapped onto an anisotropic Kondo model [11]. Increasing the electron–phonon coupling leads to a suppression of the conductance plateau width [11, 9] as a function of the gate voltage.

We study a double quantum dot (DQD) in a side-coupled configuration (figure 1), connected to a single conduction-electron channel. Similar systems have been studied using various analytical techniques such as the non-crossing approximation [12], embedding technique [13] or slave-boson mean field theory [14, 15], and recently also using more accurate numerical renormalization group (NRG) calculations [16].

In this work we study three distinct cases. In the case, already studied in detail in [16–18], where effective Coulomb interactions on DQD are positive and the intra-dot overlap is large, we find wide regimes of enhanced conductance as a function of gate-voltage at low temperatures due to the Kondo effect. Regimes of enhanced conductance are separated by regimes where localized spins on DQD are antiferromagnetically (AFM) coupled. In the limit when the dot a is only weakly coupled, the system enters the 'two-stage' Kondo regime [19, 16], where we again find a wide regime of enhanced conductivity under the condition that the high- and the low-Kondo temperatures (T_{K} and T_{K}^0 respectively) are well separated and the temperature of the system T is in the interval $T_{\mathrm{K}}^0 \ll T \ll T_{\mathrm{K}}$.

In the second case we explore the coexistence of the spin and charge Kondo state with different Kondo temperatures that are realized when there is an effective attractive interaction on one of the quantum dots. We show that spin and charge susceptibilities are screened at the corresponding spin and charge Kondo temperatures. Such a spin–charge Kondo state can be realized when two molecules, one with a strong phonon mode and the other with a localized orbital where electrons experience strong Coulomb interaction, would be coupled to metallic leads.

Finally, in the case of three side-coupled quantum dots, we demonstrate that a multi-stage Kondo effect is realized provided that exchange couplings between successive quantum dots are smaller than the corresponding Kondo temperatures.

2. Model and method

The Hamiltonian that we study reads

$$H = \delta_d(n_d - 1) + \delta_a(n_a - 1) - t_d \sum_\sigma \left(d_\sigma^\dagger a_\sigma + a_\sigma^\dagger d_\sigma\right) \tag{1}$$

$$+ \frac{U_d}{2}(n_d - 1)^2 + \frac{U_a}{2}(n_a - 1)^2 \tag{2}$$

$$+ \sum_{k\sigma} \epsilon_k c_{k\sigma}^\dagger c_{k\sigma} + \sum_{k\sigma} V_d(k)\left(c_{k\sigma}^\dagger d_\sigma + d_\sigma^\dagger c_{k\sigma}\right), \tag{3}$$

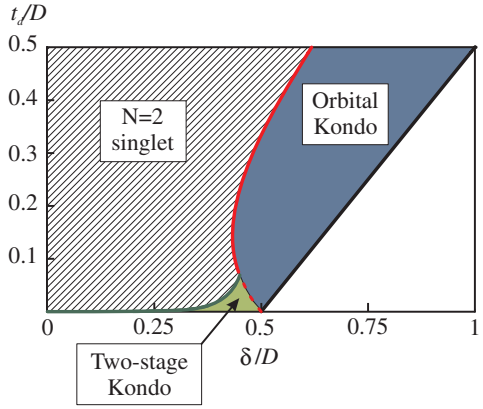

Figure 2. Phase diagram of a DQD for $U/D = 1$, obtained using analytical estimates as given in the text. The grey area represents the region of the Kondo regime where $S \sim 1/2$, $\langle n\rangle \sim 1$, and $G/G_0 \sim 1$. In the shaded area, called the spin-singlet regime, where $S \sim 0$ and $\langle n\rangle \sim 2$, the spin–spin correlation function is enhanced, i.e. $\langle \mathbf{S}_a \cdot \mathbf{S}_d\rangle \lesssim -0.5$ and $G/G_0 \sim 0$. The two-stage Kondo regime is explained further in the text.

where $n_d = \sum_\sigma d_\sigma^\dagger d_\sigma$ and $n_a = \sum_\sigma a_\sigma^\dagger a_\sigma$. Operators $d_\sigma^\dagger$ and $a_\sigma^\dagger$ are creation operators for an electron with spin σ on site d or a. On-site energies of the dots are defined by $\epsilon = \delta - U/2$. For simplicity, we choose the on-site energies and Coulomb interactions to be equal on both dots, $\delta_a = \delta_d = \delta$. Coupling between the dots is described by the inter-dot tunnelling coupling t_d. Dot d couples to both leads with equal hopping t'. As it couples only to symmetric combinations of the states from the left and the right lead, we have used a unitary transformation [20] to describe the system as a variety of the single-channel, two-impurity Anderson model. Operator $c_{k\sigma}^\dagger$ creates a conduction band electron with momentum k, spin σ and energy $\epsilon_k = -D\cos k$, where $D = 2t$ is the half-bandwidth. The momentum-dependent hybridization function is $V_d(k) = -(2/\sqrt{N+1})\, t' \sin k$, where N in the normalization factor is the number of conduction band states.

We use Meir–Wingreen's formula for conductance in the case of proportionate coupling [21] which is known to apply under very general conditions (for example, the system need not be in a Fermi-liquid ground state) with spectral functions obtained using the NRG technique [22–25]. At zero temperature, the conductance is

$$G = G_0 \pi \Gamma A_d(0), \tag{4}$$

where $G_0 = 2e^2/h$, $A_d(\omega)$ is the local density of states of electrons on site d and $\Gamma/D = (t'/t)^2$.

We use the density-matrix [25, 17] version of the standard NRG method [22]. In our NRG calculations we took into account the rotational invariance in the spin space as well as, where applicable, in the isospin space, i.e. $SU(2)_{\text{spin}} \otimes SU(2)_{\text{isospin}}$.

3. Phase diagram of the DQD system

As a part of the introduction, we first review some findings on the model with repulsive Hubbard interaction $U_d = U_a = U > 0$ as already given in [17, 18]. We first present the phase diagram of the DQD system as depicted in figure 2. The regime of high conductance is represented by the dark-grey area. High conductance is a consequence of the Kondo regime where $\langle n\rangle \sim 1$. Full lines defining the Kondo regime are given by the following analytical

expressions: $\delta_1 = t_d(2\sqrt{1+(U/4t_d)^2}-1)$ and $\delta_2 = (U/2+t_d)$. A spin-singlet regime forms in the strong coupling regime as soon as $\langle n\rangle \sim 2$, while in the weak coupling regime, i.e. for $t_d/D \lesssim 1$ the spin-singlet state persists down to the following condition $J_{\mathrm{eff}} = T_{\mathrm{K}}$. In the opposite case, when $J_{\mathrm{eff}} < T_{\mathrm{K}}$, exponentially small scale, the two-stage Kondo regime appears for $T < T_{\mathrm{K}}^0$. At low temperatures, the conductance is enhanced when $T_{\mathrm{K}}^0 \lesssim T \lesssim J_{\mathrm{eff}}$.

We now explore in detail the limit when $t_d \to 0$. In this case one naively expects to obtain essentially identical results to the single-dot case. It turns out, however, that a non-zero inter-dot coupling, $t_d \neq 0$, represents a relevant perturbation to the system in the limit $T \to 0$. A clear physical picture is obtained by comparing the two relevant energy scales: the exchange interaction J_{eff} and the single impurity Kondo temperature. In the region defined by $J_{\mathrm{eff}} < T_{\mathrm{K}}$ and $\delta < U/2$, the system enters the two-stage Kondo regime. In this regime, a gap of width T_{K}^0 opens in the density of states $A_d(\omega)$ [16] which consequently leads to a decrease of the conductance when the temperature is below T_{K}^0. The lower Kondo temperature T_{K}^0 depends exponentially on T_{K} as [16, 19]

$$T_{\mathrm{K}}^0 \sim T_{\mathrm{K}} \exp(-\alpha T_{\mathrm{K}}/J_{\mathrm{eff}}). \tag{5}$$

When by decreasing δ or by increasing t_d, the exchange interaction overcomes T_{K}, i.e. $J_{\mathrm{eff}} > T_{\mathrm{K}}$, the gap in $A_d(\omega)$ is given by J_{eff}. In this regime the two local moments on DQD form a spin-singlet.

The two-stage Kondo regime can be clearly observed in figure 3(a) where we show the impurity part of the spin susceptibility χ_{s}

$$\chi_{\mathrm{s}}(T) = \frac{(g\mu_{\mathrm{B}})^2}{k_{\mathrm{B}}T}\left(\langle S_z^2\rangle - \langle S_z^2\rangle_0\right). \tag{6}$$

The first expectation value in this expression refers to the system with the double quantum dot, while the second refers to the system without the dots. The two-stage Kondo effect manifests itself as two successive decreases of the susceptibility, first at $T \sim T_{\mathrm{K}} \sim 10^{-7}$ followed by the second at $T \sim T_{\mathrm{K}}^0$ [16]. In this case, the two-stage Kondo effect occurs for $t_d/D \lesssim 1.6\times 10^{-4}$.

The same effect can also be seen in the temperature-dependent impurity contribution to the entropy $S(T)$, defined via

$$S(T) = \frac{(E-F)}{T} - \frac{(E-F)_0}{T}, \tag{7}$$

where $E = \langle H\rangle = \mathrm{Tr}\left(H\mathrm{e}^{-H/(k_{\mathrm{B}}T)}\right)$ and $F = -k_{\mathrm{B}}T\ln\mathrm{Tr}\left(\mathrm{e}^{-H/k_{\mathrm{B}}T}\right)$. At $T \sim T_{\mathrm{K}}$ the entropy first decreases from $2\ln 2$ to $\ln 2$, see figure 3(b). This drop indicates the Kondo screening of the local moment on the dot-d while the moment on the dot-a remains unscreened and nearly free. The second drop takes place at $T \sim T_{\mathrm{K}}^0$.

With increasing δ, T_{K} increases, and the condition for the two-stage Kondo effect is satisfied at increasingly larger t_d/D. In figure 4 we present $\chi_{\mathrm{s}}(T)$ and $S(T)$ calculated at $\delta/D = 0.4$. The two-stage Kondo effect sets in at substantially larger values of t_d/D than in the $\delta = 0$ case, i.e. at $t_d/D \sim 0.01$.

In figure 5 we explore how the two Kondo temperatures are reflected in the shape of the frequency dependent spectral function $A_d(\omega)$, computed on the dot d. At $\omega \sim U/2$ all curves display a charge-transfer peak. At lower frequencies spectral functions again increase around $\omega \sim T_{\mathrm{K}}$, and then decrease around $\omega \sim T_{\mathrm{K}}^0$. All calculations were done at the effective temperature $T/D \sim 10^{-16}$, which is lower than T_{K}^0 for all t_d, except for $t_d/D \sim 10^{-8}$. Taking into account the Meir–Wingreen formula [21] for the zero-bias conductance, equation (4), we realise that in the limit $T \to 0$, $G/G_0 \to 0$ for any finite t_d/D. At small but finite T, such that $T_{\mathrm{K}}^0 \lesssim T \ll T_{\mathrm{K}}$, the gap in $A_d(\omega = 0)$ closes and the conductance approaches its unitary limit $G/G_0 \sim 1$.

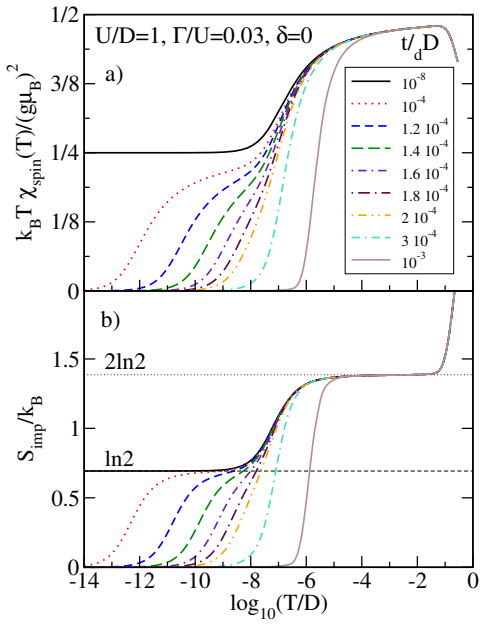

Figure 3. Temperature-dependent spin-susceptibility (a) and entropy (b) for various values of t_d/D, computed at $\delta = 0$, $\Gamma/D = 0.03$, $U/D = 1$. See also [16].

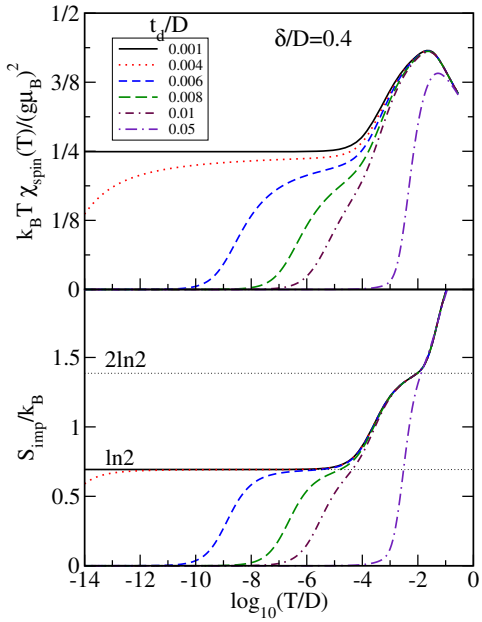

Figure 4. The same as in figure 3, except for $\delta = 0.4$.

4. Spin versus charge Kondo effect

In this section we investigate a system with $U_d = -U_a = U > 0$. The negative U on dot-a simulates the effect of strong electron–phonon interaction. Beside the impurity spin

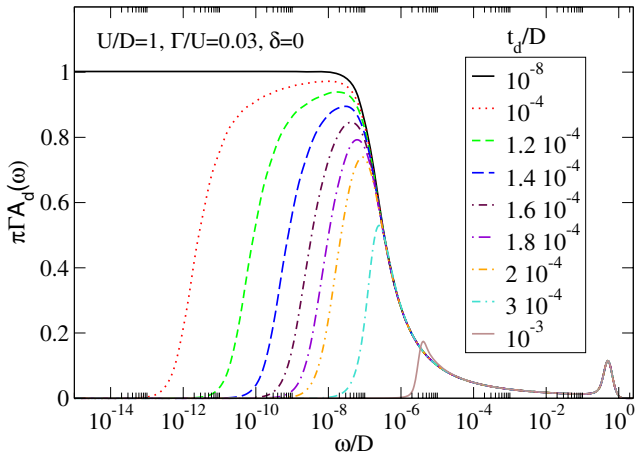

Figure 5. Normalized spectral function $A_d(\omega)$ of the DQD system. System parameters are identical to those used in figure 3. See also [16].

susceptibility and entropy we also compute the normalized charge susceptibility, defined as

$$\chi_{\mathrm{c}}(T) = \frac{1}{k_{\mathrm{B}}T}\left(\langle I_z^2\rangle - \langle I_z^2\rangle_0\right), \tag{8}$$

where I^z is the z-component of the total isospin of the system. The isospin operators are given by

$$\mathbf{I}_i = \sum_{\alpha\alpha'} \eta^\dagger_{i,\alpha}\boldsymbol{\sigma}_{\alpha\alpha'}\eta_{i,\alpha'}, \tag{9}$$

where the Nambu spinor $\eta_i^\dagger$ on the impurity orbitals are defined by

$$\eta_a^\dagger = \begin{pmatrix} a_\uparrow^\dagger \\ -a_\downarrow \end{pmatrix}, \qquad \eta_d^\dagger = \begin{pmatrix} d_\uparrow^\dagger \\ d_\downarrow \end{pmatrix}, \tag{10}$$

where the isospin raising operator is defined as $I^+ = d_\downarrow^\dagger d_\uparrow^\dagger - a_\downarrow^\dagger a_\uparrow^\dagger$. Similarly, isospin operators can be defined on the Wilson's chain and the total isospin operator can then be defined by a sum of isospin operators over all orbitals of the problem (impurities and conduction band). For $\delta = 0$, both $\mathbf{I}^2$ and I_z commute with H and I and I_z are additional good quantum numbers.

Since the system consists of two quantum dots, one with positive- and the other with negative-U, we expect that the dot-d would display a spin Kondo effect where the local spin moment would be screened by spin fluctuation in the lead, while dot-a would display a charge Kondo effect where charge degrees of freedom on dot-a would be screened by pair fluctuations in the leads. Due to different overlaps with the leads we expect the spin Kondo temperature T_{KS} to be different from the charge Kondo temperature, T_{KC}.

In figure 6 we present results of $\chi_{\mathrm{s}}(T)$, $\chi_{\mathrm{c}}(T)$ and $S(T)$ for various inter-dot coupling strengths. At large $t_d/U \gtrsim 0.3$ both susceptibilities as well as the entropy show a rapid drop with the temperature, characteristic for a system where the ground state of the DQD is a spin and isospin singlet (state with no spin or charge fluctuations). This finding is in agreement with the solution of the DQD system in the atomic limit. For $t_d > \sqrt{3}U/6 \sim 0.29U$, the ground state is nondegenerate spin and isospin singlet ($S = 0$, $I = 0$) with energy

$$E_0(S = 0, I = 0) = -2t_d. \tag{11}$$

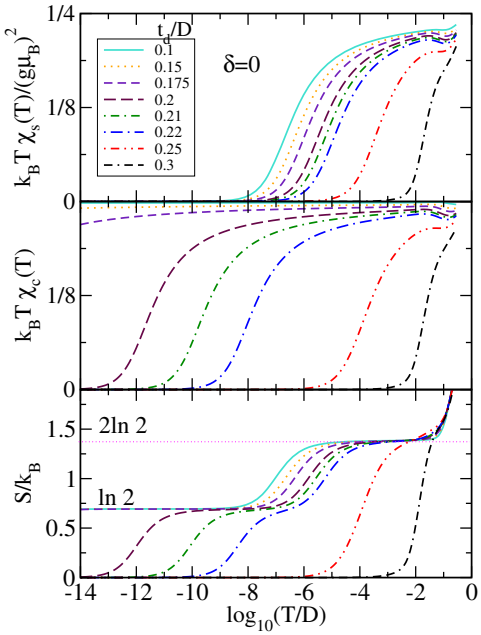

Figure 6. Temperature-dependent χ_s, χ_c and S for various values of t_d/D, computed at $\delta = 0$, $\Gamma/D = 0.03$, $U_d/D = -U_a/D = 1$.

In the opposite case, the ground state becomes a four-fold degenerate spin doublet ($S = 1/2$), isospin doublet ($I = 1/2$) with energy

$$E_0(S = 1/2, I = 1/2) = -\sqrt{t_d^2 + U^2/4}. \tag{12}$$

In the $t_d \to 0$ limit, the latter state is composed of a spin (up or down) moment on the dot-d and zero ($I_z = -1/2$) or doubly occupied ($I_z = +1/2$) dot-a. All curves in figure 6 for $t_d/D \lesssim 0.22$ show two separate Kondo screenings: the spin Kondo effect is visible in $\chi_s(T)$ at T_{KS} and the charge Kondo effect is visible in $\chi_c(T)$ at $T_{KC} < T_{KS}$. This is corroborated by the shape of $S(T)$, which shows a plateau at $2\ln 2$ at $T > T_{KS}$, in agreement with the four-fold degenerated $S = I = 1/2$ ground state, a drop at $T \sim T_{KS}$, followed by a plateau at $\ln 2$ due to the uncompensated isospin moment (degenerate zero and doubly occupied states on the dot-a), and finally a drop at $T \sim T_{KC}$. Decreasing t_d/D affects T_{KC} much more than T_{KS}. A simple explanation where the effective hybridization of the dot-a strongly depends on t_d/U while hybridization of the dot-d becomes t_d-independent for small t_d seems to be adequate.

In figure 7 we present spectral functions of the DQD system. In all figures there is a charge-transfer peak, located at $\omega = \sqrt{t_d^2 + U^2/4}$. There is an additional high-frequency peak which is, for $t_d < \sqrt{3}U/6$, located at $\omega = \sqrt{t_d^2 + U^2/4} - 2t_d$. In this regime, i.e. for $t_d < \sqrt{3}U/6$, a sharp increase in $A_d(\omega)$ at $\omega \sim T_{KS}$ signals the development of the spin Kondo peak on the dot-d, while at lower frequency $\omega \sim T_{KC}$ a gap opens in $A_d(\omega)$. In contrast, there is an additional increase of spectral weight in $A_a(\omega)$ below this frequency. In the limit of $\omega \to 0$ there is an isospin Kondo peak in $A_a(\omega)$, mirrored by a gap of width $\Delta\omega \sim 2T_{KC}$ within the spin Kondo peak in $A_d(\omega)$.

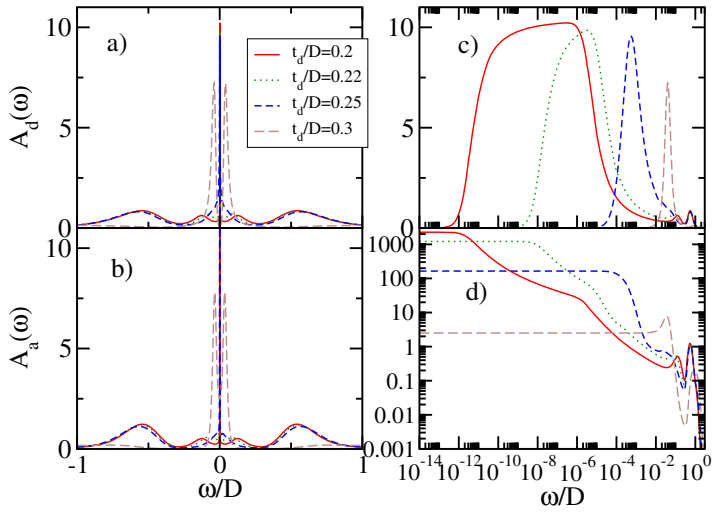

Figure 7. Spectral functions $A_d(\omega)$ ((a), (c)) and $A_a(\omega)$ ((b), (d)) of the DQD system. System parameters are identical to those used in figure 6.

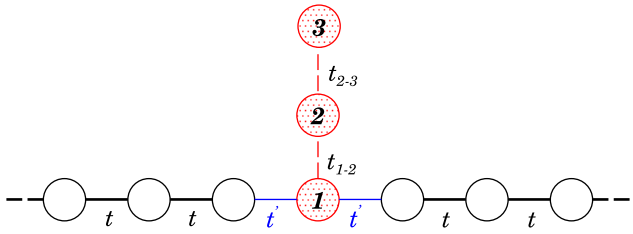

Figure 8. Side-coupled configuration of three quantum dots.

5. Three-stage Kondo model in a side-coupled TQD model

A natural question arises when studying the two-stage Kondo effect in a side-coupled quantum dot: could one realise a multi-stage Kondo effect in a series of side-coupled quantum dots. We consider the following model of three impurities, one coupled directly to a continuum and two coupled in chain to the first one. Instead of solving the more realistic three Anderson impurities model as depicted in figure 8, we solve a simplified version of three Kondo impurities:

$$H = H_{\text{band}} + \sum_i H_i + H_c + H_{123} \tag{13}$$

$$H_{\text{band}} = \sum_{k\sigma} \epsilon_k c^\dagger_{k\sigma} c_{k\sigma}\,, \tag{14}$$

$$H_i = \delta(n_i - 1) + \frac{U}{2}(n_i - 1)^2, \tag{15}$$

$$H_c = \frac{1}{\sqrt{L}} \sum_{k\sigma} V_k \left(c^\dagger_{k\sigma} d_{1\sigma} + d^\dagger_{1\sigma} c_{k\sigma} \right), \tag{16}$$

$$H_{123} = J_1 \mathbf{S}_1 \cdot \mathbf{S}_2 + J_2 \mathbf{S}_2 \cdot \mathbf{S}_3, \tag{17}$$

where $J_1 = -4t^2_{1,2}/U$ and $J_2 = -4t^2_{2,3}/U$. In the case when $J_1 < T_{\text{K}}$, where T_{K} is the single-impurity Kondo temperature of the dot-1, and $J_2 < T^0_{\text{K}}$ where T^0_{K} is the second-stage Kondo

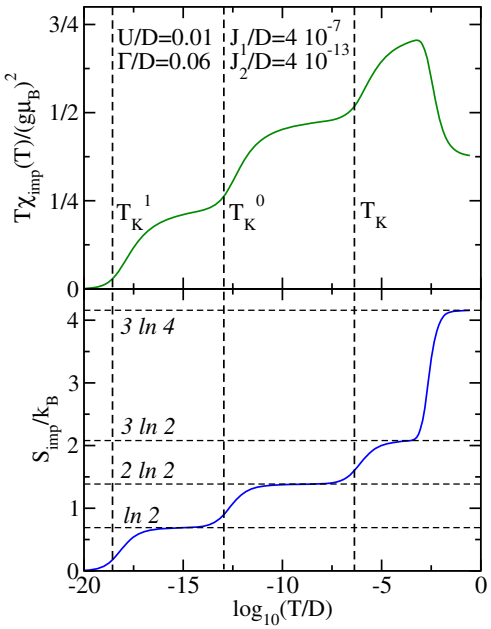

Figure 9. Temperature-dependent susceptibility and entropy for a side-coupled chain of three Kondo-like impurities.

temperature, yet another low-energy scale

$$T_{\mathrm{K}}^{1} \sim \exp(-\alpha T_{\mathrm{K}}^{0}/J_2) \tag{18}$$

appears in the problem. The system under the above conditions undergoes three $S = 1/2$ Kondo screening cross-overs, i.e. a three-stage Kondo effect, as can be seen in figure 9.

At $T \gtrsim T_{\mathrm{K}}$, there is the local moment regime where $S/k_{\mathrm{B}} \sim 3\ln 2$ and the local moment approaches $T\chi_{\mathrm{imp}}/(g\mu_{\mathrm{B}})^2 \sim 3/4$, characteristic of three noninteracting local spins. For temperatures below the first Kondo temperature, i.e. $T \lesssim T_{\mathrm{K}}$, the local moment on dot-1 couples into a singlet with conducting electrons while spins on dots-2 and 3 remain uncoupled, which gives $S/k_{\mathrm{B}} \sim 2\ln 2$ and $T\chi_{\mathrm{imp}}/(g\mu_{\mathrm{B}})^2 \sim 1/2$. There is a second drop of S and χ_{imp} at $T \lesssim T_{\mathrm{K}}^{0}$ where the spin on the dot-2 becomes screened by the quasiparticles in the leads forming a Fermi-liquid with the screened moment on the dot-1. The remains of the entropy $S/k_{\mathrm{B}} \sim \ln 2$ as well as the local moment $T\chi_{\mathrm{imp}}/(g\mu_{\mathrm{B}})^2 \sim 1/2$ in this temperature range are due to unscreened spin on the dot-3. Finally, there is a total screening of the local moment at $T \lesssim T_{\mathrm{K}}^{1}$.

The numerical renormalization group eigenvalue flow is shown in figure 10. Each Kondo screening induces an additional $\pi/2$ quasiparticle scattering phase shift while one 'free' local moment is simultaneously removed from the problem. Each $\pi/2$ phase shift corresponds to a change of the boundary condition for the conduction band electrons from periodic to anti-periodic (or vice-versa) or, from another point of view, each Kondo screening removes one conduction band site from the Wilson chain [22]. As a consequence, we observe an alternation between two sets of fixed point energies, each set corresponding to one possible boundary condition. Note that neither quantum numbers nor the degeneracy of the levels composing one *energy* level remain the same after two such alternations: this is due to the successive removal of the 'free' local moments from the problem. The degeneracy of the group of states having (approximately) the same energy decreases after each Kondo cross-over; in particular,

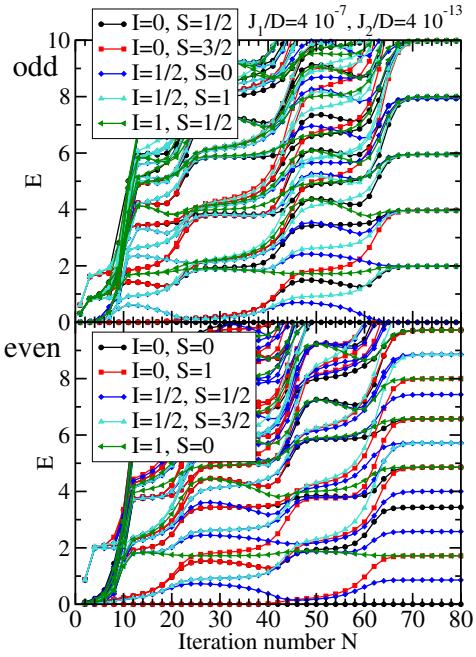

Figure 10. Numerical renormalization group eigenvalue flows for odd- and even-length Wilson chains of the side-coupled triple quantum dot system. The system exhibits three-stage Kondo screening at three different Kondo temperatures. The levels are labelled by the quantum numbers I and S, the total isospin and total spin of the system.

the eigenvalues corresponding to high total spin are pushed to higher energies. Of course, only the final strong-coupling fixed point is stable.

6. Conclusions

We have explored different regimes of the side-coupled DQD. In the case of positive Hubbard interactions when quantum dots are *strongly coupled*, wide regions of enhanced, nearly unitary conductance exist due to the underlying Kondo physics. Results were summarized in a phase diagram of the DQD structure. When DQD is doubly occupied, conductance is zero due to formation of the spin-singlet state which is effectively decoupled from the leads. When quantum dots are *weakly coupled* unitary conductance exists at finite temperatures when two electrons occupy DQD due to a two-stage Kondo effect as long as the temperature of the system is well below T_{K} and above T_{K}^{0}.

It should be noted that if the signs of *both* electron–electron interaction parameters U_d and U_a are inverted, we obtain an equivalent problem, the only change being that the roles of spin and isospin are permuted. If both quantum dots have negative U, we will thus observe enhanced conductance due to the charge Kondo effect for strong inter-dot tunnelling coupling and suitable δ, and the two-stage charge Kondo effect for weak inter-dot coupling.

We have explored a system where one of the dots is strongly coupled to phonon degrees of freedom. This effect was simulated by the introduction of an effective negative-U interaction on one of the dots, while U on the other dot was kept positive. The main goal was to explore the possibility of the coexistence of the spin and charge Kondo effect. We found out that, indeed,

spin and charge Kondo effects can coexist. Even though our model contains two leads, due to mirror symmetry the underlying problem falls into the class of the single-channel Kondo problems. It is worth stressing that as a consequence of the spin–charge separation in the leads, a single channel is sufficient to completely screen two different moments—spin as well as isospin. For $U_d > 0$, $U_a < 0$ and small t_d, the local moment (spin) on the directly coupled dot occurs at a higher spin Kondo temperature, while the isospin degree of freedom on the side-coupled dot is screened at a much lower charge Kondo temperature. For $U_d < 0$ and $U_a > 0$ the roles of the spin and charge are simply reversed: there is a charge Kondo effect on the directly coupled dot and a spin Kondo effect on the side-coupled dot.

In the case of TQD, a multi-stage Kondo effect exists for the appropriate choice of the exchange coupling constants. In the zero temperature limit, the conductance approaches the unitary limit in the particle–hole symmetric case, since the TQD fixed point is identical to the single-impurity fixed point with unitary conductance in the particle–hole symmetric point. In fact, this conclusion can be generalized in two ways. First of all, the fixed point and the quasiparticle phase shift in the case of three impurities is the same irrespective of the values of exchange constants. Depending on the exchange constants, we can either have a three-stage Kondo effect (weak exchange coupling), a $S = 1/2$ Kondo effect for an antiferromagnetic chain composed of the three impurities (both exchange constants large), or two of the neighbouring impurities couple into a local singlet, while the spin on the third impurity is Kondo screened (if one of the exchange constants is much larger than the other). The conductance is unitary in all these cases. We can also generalize our findings for the case of more than three impurities. In the case of N side-coupled quantum dots we predict unitary zero temperature conductance in the case of odd N and zero conductance for even N. For suitable exchange constants, the screening can occur in several (N or less) stages and the conductance as a function of the temperature will be non-monotonous.

Acknowledgments

The authors acknowledge useful discussions with A Ramšak and the financial support of the SRA under grant P1-0044.

References

[1] Jeong H, Chang A M and Melloch M R 2001 The Kondo effect in an artificial quantum dot molecule *Science* **293** 2221
[2] Craig N J, Taylor J M, Lester E A, Marcus C M, Hanson M P and Gossard A C 2004 Tunable nonlocal spin control in a coupled-quantum dot system *Science* **304** 565
[3] Holleitner A W, Blick R H, Huttel A K, Eberl K and Kotthaus J P 2002 Probing and controlling the bonds of an artificial molecule *Science* **297** 70
[4] Chen J C, Chang A M and Melloch M R 2004 Transition between quantum states in a parallel-coupled double quantum dot *Phys. Rev. Lett.* **92** 176801
[5] Hofstetter W and Schoeller H 2003 Quantum phase transition in a multilevel dot *Phys. Rev. Lett.* **88** 016803
[6] Hofstetter W and Zarand G 2004 Singlet–triplet transition in lateral quantum dots: A renormalization group study *Phys. Rev.* B **69** 235301
[7] van der Wiel W G, De Franceschi S, Elzerman J M, Tarucha S, Kouwenhoven L P, Motohisa J, Nakajima F and Fukui T 2002 Two-stage Kondo effect in a quantum dot at a high magnetic field *Phys. Rev. Lett.* **88** 126803
[8] Granger G, Kastner M A, Radu I, Hanson M P and Gossard A C 2005 Two-stage Kondo effect in a four-electron artificial atom *Phys. Rev.* B **72** 165309
[9] Mravlje J, Ramsak A and Rejec T 2005 Conductance of deformable molecules with interaction *Phys. Rev.* B **72** 121403

[10] Taraphder A and Coleman P 1991 Heavy-fermion behavior in a negative-U Anderson model *Phys. Rev. Lett.* **66** 2814–7
[11] Cornaglia P S, Ness H and Grempel D R 2004 Many-body effects on the transport properties of single-molecule devices *Phys. Rev. Lett.* **93** 147201
[12] Kim T-S and Hershfield S 2001 Suppression of current in transport through parallel double quantum dot *Phys. Rev.* B **63** 245326
[13] Apel V M, Davidovich M A, Anda E V, Chiappe G and Busser C A 2004 Effect of topology on the transport properties of two interacting dots *Eur. Phys. J.* B **40** 365
[14] Kang K, Cho S Y, Kim J-J and Shin S-C 2001 Anti-Kondo resonance in transport through a quantum wire with a side-coupled quantum dot *Phys. Rev.* B **63** 113304
[15] Lara G A, Orellana P A, Yanez J M and Anda E V 2004 Kondo effect in side coupled double quantum-dot molecules *Preprint* cond-mat/0411661
[16] Cornaglia P S and Grempel D R 2005 Strongly correlated regimes in a double quantum dot device *Phys. Rev.* B **71** 075305
[17] Zitko R and Bonca J 2006 Enhanced conductance through side-coupled double quantum dots *Phys. Rev.* B **73** 035332
[18] Bonca J and Zitko R 2006 Zero-bias conductance through side-coupled double quantum dots *Preprint* cond-mat/0602381
[19] Vojta M, Bulla R and Hofstetter W 2002 Quantum phase transitions in models of coupled magnetic impurities *Phys. Rev.* B **65** 140405
[20] Glazman L I and Raikh M E 1988 Resonant Kondo transparency of a barrier with quasilocal impurity states *JETP Lett.* **47** 452
[21] Meir Y and Wingreen N S 1992 Landauer formula for the current through an interacting electron region *Phys. Rev. Lett.* **68** 2512
[22] Wilson K G 1975 The renormalization group: Critical phenomena and the Kondo problem *Rev. Mod. Phys.* **47** 773
[23] Costi T A 2001 Magnetotransport through a strongly interacting quantum dot *Phys. Rev.* B **64** 241310
[24] Krishna-Murthy H R, Wilkins J W and Wilson K G 1980 Renormalization-group approach to the Anderson model of dilute magnetic alloys. i. Statis properties for the symmetric case *Phys. Rev.* B **21** 1003
[25] Hofstetter W 2000 Generalized numerical renormalization group for dynamical quantities *Phys. Rev. Lett.* **85** 1508